Formation and Spectroscopic Manifestation of Silver Clusters on Silver Bromide Surfaces

A. P. Marchetti,* A. A. Muenter, R. C. Baetzold, and R. T. McCleary

Imaging Research and Advanced Development, Eastman Kodak Company, Rochester, New York 14652

Received: January 8, 1998; In Final Form: April 24, 1998

AgBr microcrystals that have been treated with reducing agents to form small silver clusters on their surface have been examined with low-temperature optical and optically detected magnetic resonance methods. These investigations have indicated that these treatments produce two closely related Ag clusters that are spectroscopically active. One of the centers manifests itself by low-temperature emission bands at 550 and 640 nm and an absorption band at 442 nm. The other center, which absorbs at 430 nm, acts as a surface hole trap that completely changes the nature of the AgBr donor acceptor recombination. These centers are only observable on crystals with {111} faces. Spectroscopic and theoretical considerations suggest that these spectroscopically prominent centers are silver dimers in two different surface configurations.

Introduction

When silver halide (AgX) microcrystals grown in polymeric peptizing agents (e.g., gelatin) are treated with a reducing agent, the procedure is generally understood to result in small silver clusters on the AgX surface.[1−4] This process is termed reduction sensitization (R-sensitization), and it is known to increase the photographic efficiency of microcrystalline dispersions. As the first step in the photographic process, exposure of a silver halide microcrystalline dispersion to actinic radiation creates electrons and holes in the microcrystals.[1,5] The electrons, under suitable conditions, will reduce silver ions to form unique small silver clusters (latent image) that, in the presence of appropriate reducing agents, catalyze reduction of the entire microcrystal to silver, a process known as development. Part of the population of silver clusters produced by R-sensitization is thought to be functionally different from those produced by radiation.[1−4]

A variety of photographic and photophysical evidence suggests that at least some of the R-sensitization centers interact with photoholes, destroying them and, in favorable cases, creating an additional electron that can contribute to latent image formation.[1,3,4,6,7] As a result, there is an interest in applying R-sensitization to silver halide dispersions to enhance overall photographic efficiency. There is also a need to understand the nature and photophysical behavior of these silver clusters on a semiconductor surface.

Previous studies of reduction sensitization have been extensive. Many of these investigations detail the photographic consequences of using an R-sensitization agent on a particular AgX microcrystalline dispersion.[8−11] Some studies discuss the photophysical consequences of R-sensitization, such as changes in the absorption spectra, the photoluminescence spectra, the microwave photoconductivity, and the electron paramagnetic resonance spectra.[1,12−17] Other studies describe photographically based tests for the presence of R-sensitization. One common test is gold bathing, in which a coated AgX dispersion is bathed in a labile gold solution before light exposure.[18] This produces an increase in the fraction of the AgX dispersion that develops in the absence of light, and that fraction has been found to be proportional to the level of R-sensitization.

TABLE 1: Microcrystalline Dispersions Examined

dispersion	morphology	halide	size[a] (μm)	surface area[b] (m^2/mol Ag)
T394	tabular	AgBr	2.88 × 0.087	710
T454	tabular	AgBr	2.80 × 0.078	780
T4241	tabular	AgBr	1.40 × 0.084	770
T540	tabular	AgBr	1.76 × 0.122	540
O286	octahedron	AgBr	0.79	270
C284	cube	AgBr	0.68	260
C2266	cube	AgBr	0.38	460
C712	cube	AgBr	0.06	2900
C96−PVA	cube	AgBr	0.08	2180
C128−PVA	cube	AgCl	0.07	2210
CO582	cubo-octa	AgBr	0.80	260

[a] Tabular microcrystals are characterized by an equivalent circular diameter and a thickness, octahedra by an octahedral edge length, cubes by their edge length, and cubooctahedron by an equivalent circular diameter. [b] Surface areas calculated from measured crystal size.

The intent of this paper is to detail new optical spectroscopic manifestations of silver cluster formation on AgBr microcrystals. The goal is to define, as much as possible, the nature and function of the various R-sensitization centers. To that end, low-temperature optical emission and absorption techniques, optically detected magnetic resonance methods (ODMR), and some photographic tests have been applied to dispersions of silver halide microcrystals to detect and probe the centers created by reduction sensitization. Computational methods have also been used to examine the behavior of small silver clusters on an AgBr surface.

Experimental Section

Silver Halide Dispersions, Sensitization, and Coating. The silver halide dispersions studied are summarized in Table 1, together with information on their halide content, morphology, and size. These silver halide dispersions were all made by controlled addition of solutions of $AgNO_3$ and NaBr (or NaCl) to a stirred reactor, which contained gelatin or poly(vinyl alcohol) (PVA) in water, at a temperature between 55 and 70 °C. The silver ion concentration, temperature, and pH were

* Corresponding author. Fax: (716) 722-5612. Email: apm_ekrl@kodak.com.

S1089-5647(98)00729-9 CCC: $15.00
Published on Web 06/11/1998

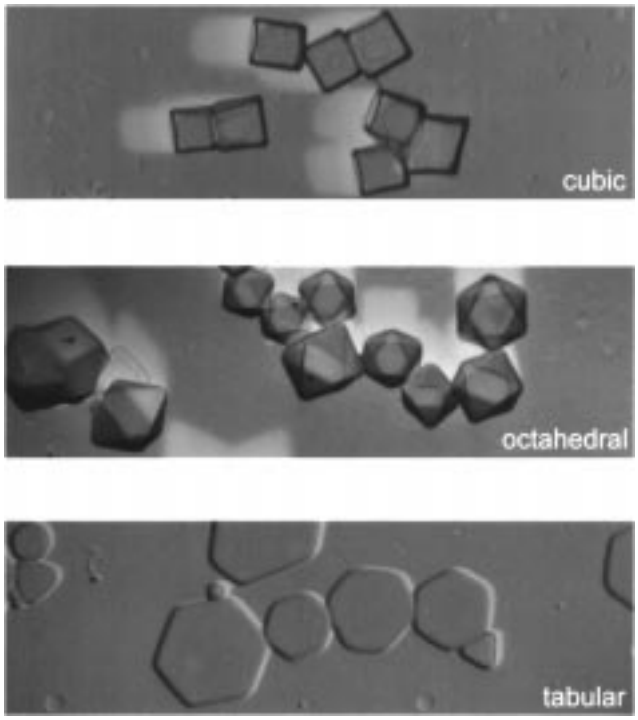

Figure 1. Shadow transmission electron micrographs of some of the cubic, octahedral, and tabular AgBr microcrystals used in this investigation.

controlled during this precipitation process. Dispersions with the suffix PVA were precipitated in that polymer; all others were precipitated in gelatin. For AgBr, cubic morphologies are obtained at higher silver ion concentrations (10^{-7} M), while octahedra are produced at lower silver concentrations (10^{-10} M). The details of the fabrication procedures have been published elsewhere.[19] Transmission electron micrographs of carbon replicas of the several silver halide morphologies used in this investigation are shown in Figure 1. The cubic morphologies have {100} surfaces, and the octahedral and tabular morphologies have {111} surfaces. AgBr microcrystals with a tabular morphology were chosen for most of the spectroscopic examples as these materials have a larger surface-to-volume ratio and at constant surface coverage gave stronger signals. The microcrystal sizes are determined by both scanning electron microscopy (SEM) and transmission electron microscopy (TEM). The TEMs are of the carbon replicas that occur after shadowing with a metal (usually Pd) and then carbon coating and then dissolving the silver halide.

R-sensitizations were accomplished by adding the reducing agent of interest to a melted silver halide dispersion (generally at 1−2 M in silver halide). The silver ion concentrations of the melted dispersions were measured with a silver electrode versus a standard Ag/AgCl electrode and characterized by the measured potential (VAg). These liquid dispersions (melts) had VAgs near 95 mV and pHs of 5.8 at 40 °C. Unless otherwise indicated, all samples were then given a heat treatment for 20 min at 60 °C. After the sensitization, a small aliquot of the microcrystalline dispersion was reserved for the luminescence studies. Melts for coating were then prepared at a VAg of about 85 mV and a pH of 6.0. These melts were coated on an acetate support to give simple coatings that could be developed in a black and white developer. These coatings had a silver laydown of 3.23 g/m^2, a gelatin laydown of 4.3 g/m^2, and a gelatin overcoat of 1.08 g/m^2. The gelatin in the coatings was cross-linked (hardened) using 1,1′ [oxybis(methylenesulfonyl)]bisethene at a level of 1.8 wt % of total gelatin.

Hydrogen sensitization of a melted sample of the AgBr tabular dispersion (T540) was carried out by placing a 50 g sample in a stainless steel vessel in a standard hydrogenation reactor, heating to 40 °C, and subjecting the sample to H_2 at 50 psi for 3 h. A sample of this hydrogen-treated microcrystalline dispersion was taken for luminescence measurements.

Redox buffers were used for preliminary studies of the oxidation of R-sensitization centers on a sample of the melted AgBr tabular dispersion T454, which had been R-sensitized with 2 mg $SnCl_2$/mol Ag. Phthalated gel at a level of 30 g per mol of Ag was added to the dispersion, which was then diluted with H_2O to a weight of 3 kg per mol of Ag. The samples were degassed by bubbling with N_2 while moderately stirring at 40 °C. Degassing and stirring continued during the redox buffer treatment, which was initiated by adding 15 mL of the redox buffer to the sample. After a 40−80 min equilibration, samples were centrifuged and washed at least once. The resulting "pellet" was used for the luminescence measurements. In these experiments, redox buffers with positive potentials (195, 450 mV) were obtained by varying mixtures of Fe^{II} and $Fe^{III}(CN)_6$ solutions, and a −80 mV solution was obtained by a mixture of Fe^{II} and Fe^{III} with EDTA. The buffer solution potentials were measured versus an Ag/AgCl reference electrode.

Photographic Testing. Standard photographic exposure of the AgX dispersions coated on acetate support was for 1 s at 365 nm through a stepped neutral density filter. The exposed coatings were developed for 20 min in an Elon-ascorbic acid developer (EAA-1).[20] The characteristic photographic response of a coated emulsion is obtained by measuring the silver optical density at each exposure level after development. A smoothly varying curve of density versus exposure is fitted to these values. The minimum density (*D*-min) is defined as the density at zero exposure, and the speed is defined as the exposure required to produce a developed density that equals the *D*-min plus 0.15 OD units. For high levels of R-sensitization, the coatings would develop almost completely to their maximum density (*D*-max) without light exposure.

Low-Temperature Luminescence and ODMR. Low-temperature luminescence spectra and lifetimes were obtained on small samples of the AgX-gelatin dispersion placed in a sample holder in a metal double Dewar.[21] The sample temperature was controlled by the flow of helium from the liquid reservoir into the sample chamber and by heaters on the expansion block and the sample holder. The sample temperature was measured with a calibrated temperature-sensitive silicon diode mechanically held to the back of the metal sample holder. The temperature readings from the diode are periodically checked with the sensor immersed in boiling helium and boiling nitrogen. Except where noted in the temperature dependence studies, the measurements were made at 6 K.

Luminescence spectra were obtained by exciting the sample with light from a helium−cadmium laser (442 and 325 nm) or a xenon lamp and monochromator. The emission was collected and chopped and then directed into a computer-controlled 1 m monochromator/photomultiplier. The spectra were corrected for the monochromator/photomultiplier response. Excitation spectra were obtained by monitoring the luminescence intensity at a specified wavelength while scanning the excitation monochromator. Excitation spectra were corrected for the lamp/monochromator variations by diverting a small fraction of the exciting light to a silicon diode of known response and dividing the spectral intensities by the diode output corrected for the diode response.

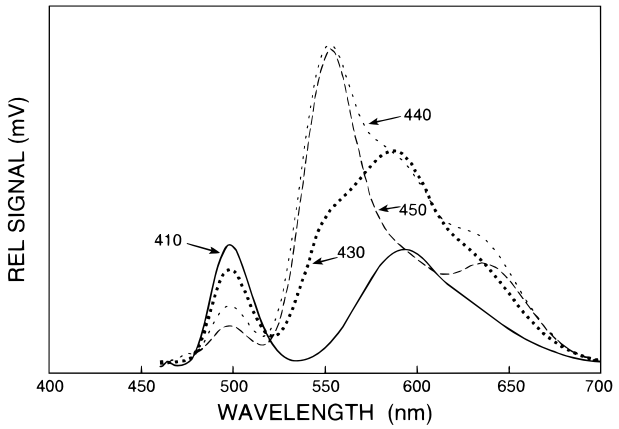

Figure 2. Emission spectra of T394 at 6 K after R-sensitization with 2 mg $SnCl_2$/mol Ag (14×10^{-9} M/m^2). The four spectra are for excitation at 410, 430, 440, and 450 nm. Note the dominance of the 550 and 640 nm bands with 440 and 450 nm excitation.

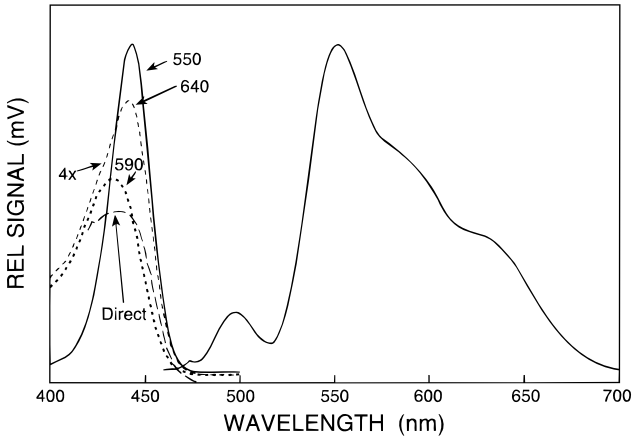

Figure 3. Emission spectrum and excitation spectra at 6 K of T394 with an R-sensitization of 2 mg $SnCl_2$/mol Ag. The emission spectrum is for 442 nm excitation, and the excitation spectra are for monitoring wavelengths of 550, 590, and 640 nm. Note the excitation spectra have peaks at about 442 nm for monitoring wavelengths of both 550 and 640 nm, while monitoring at 590 nm produces a peak at about 430 nm. The direct absorption spectrum is also shown.

Luminescence lifetimes were measured after pulsed excitation from a nitrogen laser or a nitrogen laser pumped dye laser. The pump pulse width is 0.5 ns (fwhm). The system response time is 7 ns. The response of the apparatus used to measure luminescence decays is periodically checked against known samples in the microsecond and nanosecond regions. The decay curve is the average of an accumulation of several (usually 64) decay responses.

Optically detected magnetic resonance measurements were obtained with the sample in a liquid helium Dewar, positioned in a split coil superconducting magnet that provides optical access and fields up to ~2 T. Sample temperatures below 4.2 K were obtained by pumping on the helium chamber. Typical sample temperatures were between 1.7 and 1.8 K. The sample was positioned at the end of a waveguide connected to a Klystron, which provides microwave radiation at 34 or 36 GHz. The microwave radiation was modulated at audio frequencies (150 to 10 000 Hz). Optical excitation was provided by a helium−cadmium laser or a tunable argon ion laser. The emission was collected by a lens through appropriate filters and directed onto a photomultiplier (PMT) or into a monochromator and PMT. The output from the PMT was fed into a lock-in amplifier, which was referenced to the microwave modulation frequency. A computer was used to collect and display the data from the lock-in amplifier and to control the magnetic field.

Absorption Spectra. Low-temperature absorption spectra were obtained on thin layers of R-sensitized silver halide dispersions with single-beam measurements. The reference sample was the emulsion without R-sensitization. The ratio of the light intensity from the treated sample to the untreated gives the transmission. In addition, standard room-temperature absorptance spectra (1-T-R) were measured for all of the coated samples.

Characteristics of R-Sensitizations

AgBr Tabular Microcrystals. R-sensitization occurs as a result of the reaction of one of a number of chemical reducing agents with a dispersion of AgX microcrystals or during treatments of such dispersions with increases in pH and VAg. Spectroscopically, R-sensitization manifests itself by new emission bands that occur at 550 and 640 nm. The appearance of these bands is highly dependent upon the excitation wavelength as shown in Figure 2. Excitation at 410 nm of a dispersion of AgBr microcrystals (T394) treated with 2 mg/Ag mol of $SnCl_2$ gives rise to the "normal" AgBr emission.[22,23] The "normal" emission from untreated AgBr has peaks at 495 and 590 nm due to the recombination of excitons bound to impurity iodide ions (usually at the ppm level) and donor−acceptor recombination, respectively. Excitation at shorter wavelengths, such as 325 nm, gives a similar emission spectrum. However, as the excitation wavelength is lengthened beyond 410 nm, profound changes occur. For excitation between 440 and 450 nm, the major peaks in the emission now occur at 550 and 640 nm. Excitation beyond 450 nm shows a decrease in emission intensity.

The changes in the emission spectra with changes in the excitation wavelength imply that there should be a feature associated with R-sensitization in the luminescence excitation spectrum. This spectrum for an untreated sample when monitoring emission at 500 or 590 nm shows *no* peak in the region beyond 400 nm, just a rising intensity (as 400 nm is approached) indicative of an indirect transition.[24] However, for a sample treated with 2 mg $SnCl_2$/mol Ag, bands appear in this region. Figure 3 shows the emission spectrum for 442 nm excitation and the excitation spectra when monitoring the emission at 550, 590, and 640 nm. The excitation spectra with monitoring wavelengths of 550 and 640 nm are identical, peaking at 442 nm. This indicates that these two emission peaks arise from the same absorbing state. The intensity differences for the two spectra reflect differences in the emission intensity.

To confirm the presence of absorption at wavelengths beyond the AgBr indirect edge, low-temperature direct absorption spectra of R-sensitized T394 were obtained for samples with 2 and 20 mg $SnCl_2$/mol Ag. Examination of the spectrum for the 2 mg level, shown in Figure 3, confirms an absorption peak at ≈440 nm. At the higher level of R-sensitization, the low-temperature absorption peak broadens slightly and there are indications of a very weak absorption between 470 and 480 nm. At this level of sensitization, small increases in absorptance in the 400−480 nm region can also be observed in the room-temperature spectrum of the coated microcrystals. Absorption at 470−480 nm has been observed by other investigators in the room temperature reflection spectrum of heavily R-sensitized AgX microcrystals.[1,15]

The excitation spectrum that arises with a monitoring wavelength of 590 nm is different from that of an untreated microcrystalline dispersion of AgBr and shows a peak at 430

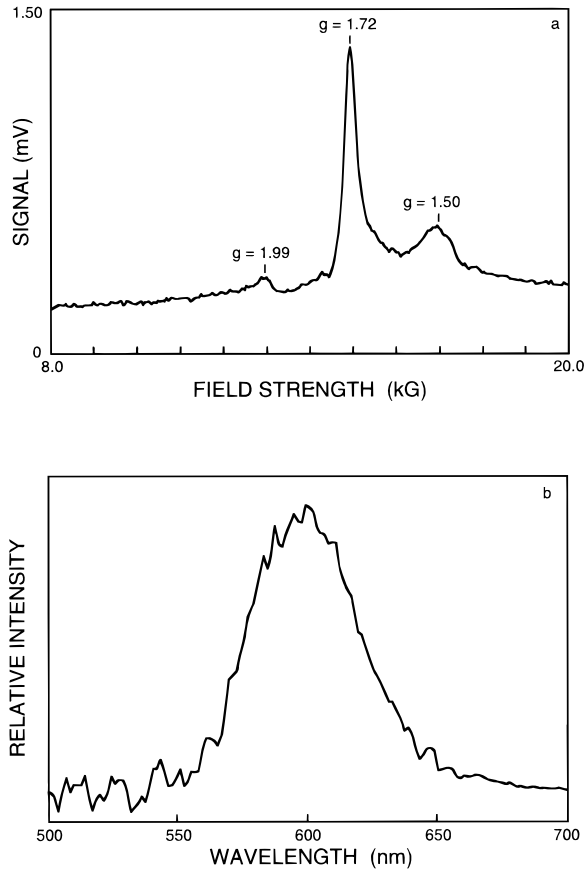

Figure 4. (a) ODMR spectrum of T4241 sensitized with 1 mg/mol Ag of tBuAB (6×10^{-9} M/m^2). The temperature was 1.7 K, microwave frequency was 36.01 GHz, microwave modulation frequency was 700 Hz, and excitation wavelength was 442 nm. The monitoring wavelength was 580 nm in the upper spectrum (a). (b) ODMR emission wavelength dependence of T394 R-sensitized with 2 mg $SnCl_2$/mol Ag, which had a ODMR spectrum very similar to T4241. The lower spectrum (b) was generated by focusing the emitted light on a monochromator and scanning the wavelength with the magnetic field set at the value corresponding to the $g = 1.72_3$ peak.

nm, a shift to slightly shorter wavelength compared to the spectrum obtained when monitoring at 550 or 640 nm in the R-sensitized sample (see Figure 3). This indicates that the R-sensitization treatment has either changed the nature of the "intrinsic" 590 nm emission or created a new, stronger emission in this region. Note that the excitation spectra observed when monitoring the iodide-bound exciton emission (470−510 nm) do not exhibit a band at 430−440 nm in the R-sensitized samples. These spectra are the same as those previously published for untreated samples.[25]

This change in the character of the 590 nm band has been confirmed by optically detected magnetic resonance (ODMR) spectra of R-sensitized microcrystals. AgBr crystals and microcrystalline dispersions have a characteristic ODMR spectrum.[22] With 34−36 GHz microwaves, four peaks are observed in single crystals of AgBr at *g*-factors ($h\nu = g\beta H$) of 2.08_5, $\approx 1.81_4$, $\approx 1.79_4$, and 1.49_3. This ODMR spectrum has been interpreted as arising from donor acceptor radiative recombination. These resonances have been assigned to acceptor, intermediate case exciton, intermediate case exciton, and donor resonances, respectively.[22] The R-sensitized microcrystals have a very different ODMR spectrum, as shown in Figure 4a. The R-sensitized samples have a resonance at $g = 1.99$, a relatively sharp resonance at $g = 1.72_3$, and a broad but pronounced resonance, which peaks at g $\approx$ 1.50, the donor or shallowly trapped electron resonance region. The ODMR signals originate from the ≈590 nm emission. This is shown in Figure 4b where the intensity of the ODMR signal at $g = 1.72_3$ is monitored as a function of the emission wavelength. The same wavelength dependence was observed with the ODMR signals at $g = 1.99$ and at $g = 1.52$ near the donor resonance. The ODMR signal intensity clearly peaks at, or near, 590 nm. The modulation frequency dependence for the R-treated samples is also different from that of untreated microcrystals, a result that indicates a difference in emission lifetime in the two types of samples. The R-sensitized samples exhibit no observable ODMR signals when the monitoring wavelength is 550 nm. The ODMR spectrum obtained with a monitoring wavelength of 650 nm still has a strong $g = 1.72_3$ resonance, but the donor resonance is severely broadened and shifted to lower *g*-values. A weak and broadened signal from the instrinsic acceptor resonance at $g = 2.08$ is also evident along with the resonance at $g = 1.99$.

TABLE 2: Lifetime for the Iodide-Bound Exciton and Half-Lives of the Emission Bands for an AgBr Tabular Dispersion Sensitized with Varying Levels of $SnCl_2$

level of $SnCl_2$	decay constants for various emission wavelengths			
	500 nm[a]	550 nm[b]	590 nm[b]	640 nm[b]
none	19 μs		9 μs	
2 mg/mol Ag		<10 ns	3 μs	≈10 (10, 110) μs[c]
20 mg/mol Ag		<10 ns	8 μs	≈12 (10, 100) μs[c]

[a] Lifetime. [b] Half-time. [c] Data in parentheses are two-component lifetimes.

The luminescence decay after pulsed excitation has previously been examined and documented for AgBr.[26] The iodide-bound exciton with an emission peak at 495 nm has a single-exponential decay in the bulk of 16 ± 3 μs.[23,27] The donor−acceptor emission, which peaks at 590 nm, exhibits a hyperbolic decay (sum of many exponential decays) that has a half-decay time of about 10 μs depending on impurity levels.[26] The new emission bands at 550 and 640 nm in R-sensitized AgBr, as well as the modified 590 nm band, each exhibit different decay courses. The 550 nm band has a very short decay time (<10 ns), which may be exponential. The decay of the "modified" 590 nm donor−acceptor emission and the 640 nm emission both show hyperbolic decays. The decay of the 640 nm band can also be "decomposed" reasonably well into two exponentials. The decay constants are summarized in Table 2.

The change in the luminescence of a silver halide microcrystalline dispersion that has been treated with a reducing agent is also dependent on the concentration of reducing agent used. This is illustrated in Figure 5 with the emission spectra that occur with 442 nm excitation and various levels of $SnCl_2$ applied to the AgBr tabular microcrystal T394. It is important to note that although the lowest level of $SnCl_2$ used (0.02 mg/mol Ag) produces only very small, if any, changes in the emission, the excitation spectrum from this sample clearly shows a peak at 442 nm when the emission is monitored at 550 nm. The 550 nm emission is clearly visible at 0.2 mg/mol Ag, and this band becomes the dominant feature of the spectrum at 2 mg/mol Ag and above. The 640 nm band also becomes pronounced at these levels.

The reducing agent $SnCl_2$ used to produce the luminescence and absorption changes detailed above has commonly been used as an R-sensitization agent and would be expected to change the photographic behavior of coated AgBr tabular microcrystals. This expectation was confirmed in photographic experiments on coatings derived from the sensitized microcrystalline dispersions whose spectra are shown in Figure 5. The photographic

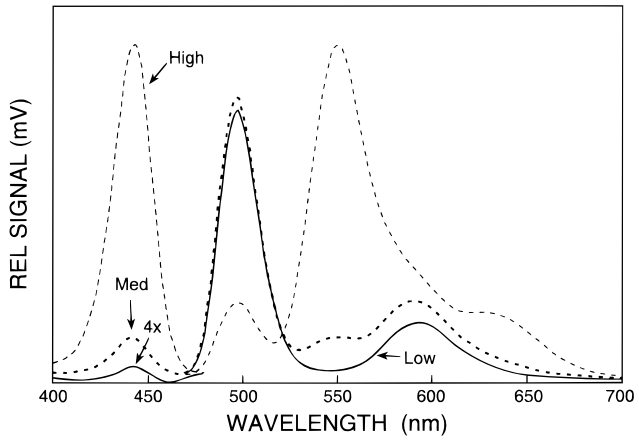

Figure 5. Emission spectra for T394 treated with different levels of $SnCl_2$. The temperature was 6 K, and the excitation wavelength was 442 nm. The levels of $SnCl_2$ were 0.02, 0.2, and 2.0 mg/mol Ag, and these levels correspond to 0.14, 1.4, and 14×10^{-9} M/m^{2,} respectively. The excitation spectra are shown for a monitoring wavelength of 550 nm.

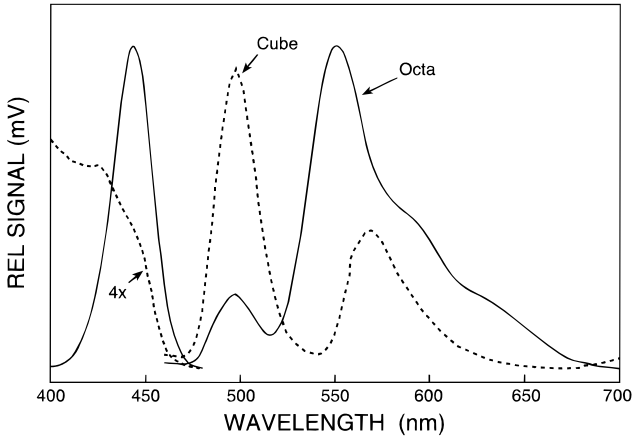

Figure 6. Emission and excitation spectra at 6 K for C284 and O286, cubic and octahedral microcrystalline dispersions treated with 7.8 mg $SnCl_2$/mol Ag (150 and 130×10^{-9} M/m^2, respectively). The excitation wavelength was 442 nm, and the monitoring wavelength was 550 nm. The excitation spectrum for C284 was scaled up by a factor of 4.

speed increased by a factor of 2 for treatment with 0.02 mg $SnCl_2$/ mol Ag, by a factor of 5 for 0.2 mg $SnCl_2$/mol Ag, and by a factor of 6 for 2.0 mg $SnCl_2$/mol Ag. All of these sensitivity increases occurred with essentially no increase in the developed density with no light exposure (*D*-min). However, the coating with the highest level of $SnCl_2$ (20 mg/mol Ag) reached the maximum possible developed density (*D*-max) even without exposure to light. It is interesting to note that 2.0 mg $SnCl_2$/mol Ag is theoretically capable of producing about 20 000 Ag atoms/μm^2 of microcrystal surface, assuming two Ag atoms are produced from the oxidation of each $SnCl_2$ molecule.

The discussion to this point has centered on the spectroscopic and photographic changes produced by use of $SnCl_2$ as a reduction sensitization agent. Identical changes are produced by other reducing agents such as *tert*-butylamine borane (tBuAB), dimethylamine borane (DMAB), and thiourea dioxide. Manipulation of pH and VAg has also frequently been used to produce changes in photographic speed attributed to R-sensitization.[28] To investigate the effect of such changes on the luminescence spectra, samples were adjusted to various elevated values of pH and/or VAg and heated for 20 min at 60 °C before returning to the original pH and VAg values. These experiments indicated, as expected, that high silver ion concentrations and high pHs gave all of the manifestations of R-sensitization. The spectroscopic signals for R-sensitization occurred at pHs above ≈9.5 with VAgs above ≈200 mV.

Treatment of coatings of dispersed AgX microcrystals with H_2 is also known to give increases in photographic sensitivity.[2,29] A 3 h H_2 treatment of a melted sample of dispersion T540 gave luminescence emission and excitation identical to those shown in Figure 5 for an intermediate level of $SnCl_2$. Spectra of the control samples, where the silver halide dispersion was untreated or simply heated at 40 °C for 3 h, showed no evidence of the emission at 550 and 640 nm nor of the excitation peak at 442 nm.

Attempts were made to create the R-sensitization signals by exposing samples of AgBr tabular dispersions to light. The samples were exposed on a benchtop to room lights for 10 and 1000 s. The samples were then placed in a cryostat and the temperatures reduced to 6 K. Samples treated in this manner showed no R-sensitization signal, but they did exhibit an apparent reduction in the intrinsic emission intensity. In addition, several samples were exposed with a nanosecond time scale flash. Excitation spectra for these samples showed a weak peak at about 440 nm.

AgBr Octahedral and Cubic Microcrystals. Up to this point only the spectroscopic manifestations of the application of R-sensitization to AgBr tabular microcrystals with {111} surfaces have been detailed. As might be expected, similar luminescence bands are observed for AgBr octahedral microcrystals. Figure 6 illustrates this similarity, showing the emission and excitation spectra for an 0.79 μm octahedral microcrystalline dispersion (O286) sensitized with 7.8 mg/mol Ag of $SnCl_2$, an amount per molar surface area equivalent to the 20 mg level used on the AgBr tabular microcrystalline dispersions discussed above. The ODMR spectrum of O286 with R-sensitization is very similar to the spectrum shown in Figure 4a.

The results differ for 0.68 μm AgBr cubic microcrystals with {100} surfaces as is illustrated in Figure 6. The figure shows that the 550 and 640 nm bands are absent in a cubic AgBr microcrystalline dispersion (C284) R-sensitized with 7.8 mg $SnCl_2$/mol Ag. This absence is not due to a shift in wavelength of the peak in the excitation spectra as a broad range of excitation wavelengths between 325 and 600 nm were explored. Further, the excitation spectrum of the 590 nm donor acceptor emission is not changed by the presence of the R-sensitization. The ODMR spectrum of R-sensitized C284 is the same as an untreated sample of this dispersion. The direct absorption spectrum was also examined at low temperature with no indication of the absorption band peaking at 442 nm that was found in R-sensitized microcrystals with {111} surfaces. The absence of the excitation and emission bands is not correlated to the photographic consequences of R-sensitization because this treatment gives a significant increase in photographic speed for the cubic microcrystalline dispersion.

Further insight into the luminescence properties of R-sensitized AgBr microcrystals with a cubic morphology can be gained by exploring a broader range of such microcrystalline dispersions. The cubic dispersion (C284) used in the example above was made at 200 mV. This precipitation condition produces well-formed cubes with sharp edges. When an 0.38 μm "cubic" dispersion (C2266) made at ≈130 mV was examined after R-sensitization, a modest 550 nm band was observed in the emission and a relatively intense excitation peak was observed. Cubic microcrystals made under these conditions have rounded edges and thus contain surfaces that are not {100}.

Smaller rounded cubes (C712) made at 130 mV in gelatin also exhibit the "characteristic" emission and excitation bands upon R-sensitization. However, a similar dispersion of small AgBr microcrystals made with poly(vinyl alcohol) (C96-PVA) as the peptizing agent, which creates very "sharp" cubes, displayed no 550 or 640 nm emission upon R-sensitization. Further, no R-sensitization-related luminescence or direct absorption was observed on small well-formed AgCl cubes (C128-PVA) grown with poly(vinyl alcohol) as a peptizing agent. The conclusion is that the 550 and 640 nm emission bands are associated with a type of silver center that does not form on {100} surfaces.

An AgBr cubooctahedral microcrystalline dispersion was also examined for R-sensitization response when sensitized with $SnCl_2$. The changes in the emission spectrum and the excitation spectrum paralleled the changes observed with an octahedral microcrystalline dispersion. The only difference was a reduction in signal magnitude for a given level of R-sensitization agent. These observations are also consistent with the assignment of the 550 and 640 nm emission bands to the presence of R-sensitization centers on surfaces that are not {100}.

The decay rate in the donor−acceptor region (590 nm) of an R-sensitized and an untreated cubic microcrystalline dispersion (C284) was also examined. The decay profiles appear nonexponential (hyperbolic) but are different in the two samples. The half-decay time in the R-sensitized sample is shorter than in the non-R-sensitized dispersion. These results suggest that the nature of the donor−acceptor emission has been modified in the cubic microcrystals. However, ODMR investigation of this R-sensitized cubic microcrystalline dispersion found *no* new resonances, but only weak signals typical of an untreated microcrystals. These data again suggest that the spectroscopically active R-sensitization centers are formed only on non-{100} microcrystal surfaces.

Temperature Dependences. The various emission bands in R-sensitized and untreated AgBr microcrystals are all expected to have different intensity−temperature profiles, depending upon the halide type and the species undergoing radiative decay. For example, the iodide-bound exciton consists of a hole bound to an impurity iodide, which then binds an electron in a hydrogenic orbital.[24] The binding energy for the electron is on the order of 30 meV, and thus the loss of this emission band between 40 and 60 K is consistent with this binding energy. In R-sensitized AgBr, both the donor−acceptor emission and the bands due to R-sensitization are lost between 60 and 80 K indicating somewhat more stable centers than the iodide-bound exciton.

Removal of R-Sensitization Centers. The photographic effects of R-sensitization can be removed by various chemical treatments, which are thought to oxidize the Ag centers associated with the sensitization. Several of these treatments were applied to an AgBr tabular microcrystalline dispersion R-sensitized with 0.4 mg/mol Ag of $SnCl_2$. Raising the hydrogen ion concentration to pH 2 and holding for 20 min at 60 °C did not change the spectroscopic signatures. Treatment with 4,4′-phenyl disulfide diacetanilide at levels between 20 and 100 mg/mol Ag removed the 550 and 640 nm emission bands.[30] The use of bis(2-amino-5-iodopyridine-dihydroiodide) mercuric iodide at 2.0 mg/mol Ag reduced the spectroscopic signatures to very low levels.[30,31] When the luminescence emission associated with R-sensitization centers and the corresponding excitation spectrum disappeared, all photographic effects of the R-sensitization were also removed.

For the AgBr tabular dispersion T454 R-sensitized with a higher level of $SnCl_2$ (2.0 mg/mol Ag), treatment of the liquid dispersion with various redox buffers also removed the R-sensitization signals in a manner dependent on the buffer potential.[1] Tests with the R-sensitized microcrystalline dispersion buffered at −80, +195, and +450 mV indicated that buffering at −80 mV decreased the intensity of the 590 nm emission relative to the 550 and 640 emissions. All luminescence associated with R-sensitization was removed when the samples were buffered at +195 and +450 mV.

Another way to remove R-sensitization centers is to expose the samples to red light.[32] R-sensitized (2 mg $SnCl_2$/mol Ag) samples of an AgBr tabular dispersion (T394) were exposed for 1 h at room temperature to the output of several diode lasers. These lasers had wavelengths of 633 nm (1.96 eV), 670 nm (1.85 eV), and 780 nm (1.59 eV) and nominal outputs of 3, 10, and 40 mW, respectively. The prominent R-sensitization luminescence emission bands at 550 and 640 nm were reduced by a factor of ≈5 for a 1 h exposure at 633 nm. Exposure at 670 nm reduced these bands by only 25%. Exposure to 780 nm radiation left the emission spectrum unchanged. These data suggest that there is a light-driven process that has a threshold at wavelengths between 670 and 780 nm and that removes the center responsible for the 442 nm absorption.

Discussion

New low-temperature photoluminescence arises from the presence of low levels of R-sensitization on AgX microcrystalline dispersions with {111} surfaces, and the photographic consequences of R-sensitization correlate with those luminescence intensities. The initial R-sensitization studies were all performed with $SnCl_2$ as the reducing agent. Similar luminescence and photographic results were found for R-sensitization by DMAB, tBuAB, thiourea dioxide, hydrogen gas, and coupled high VAg-pH treatments. The existence of common spectroscopic features from a variety of chemistries indicate that the new luminescence bands arise from the products of reduction, not the remnants of the reducing agent.

Simply exposing the AgX microcrystalline dispersions to low-intensity white light did not create the new luminescence bands. However, the spectra from samples that were exposed with a high-intensity nanosecond light pulse suggest that small numbers of the silver centers absorbing at 442 nm may be created under this condition, which is thought to create a larger number of small centers. At low intensities, it is probable that light-created clusters tend to grow in size and not in number with increasing exposure.[5]

Silver bromide octahedra gave low-temperature luminescence bands that were very similar to those found for the tabular AgBr microcrystals. Cubic AgBr microcrystals, however, gave no new luminescence peaks upon R-sensitization even though the R-sensitization produced the same photographic behavior that was observed in dispersions of AgBr microcrystals with {111} surfaces. New luminescence features were also not observed on well-formed AgCl microcrystals with {100} surfaces. This result indicated that the new luminescence features are associated with a species that does not form, or for some reason is not observable, on an R-sensitized {100} surface.

The normal donor−acceptor luminescence that is observed at 590 nm in AgBr is substantially modified by the presence of surface R-sensitization. This is shown in the ODMR spectra where the intrinsic acceptor and the intermediate case exciton resonances are replaced with new resonances at $g = 1.99$ and $g = 1.72_3$ and the donor resonance is severely broadened and possibly shifted. The g-factors for Ag_2^+ have been obtained in frozen H_2SO_4 and organic glasses.[33] They are $g_{||} = 2.001$ and

TABLE 3: Predicted Upper Limit for the Peak Positions of Smaller Silver Clusters on an AgBr Surface Assuming Dispersive Interactions[a]

cluster	0.0 (gas), eV	peak (Ar), eV	peak (AgBr surface) eV	peak (AgBr surface) nm
Ag	3.664/3.778			
Ag_2	2.849	3.18	<2.98	>416
Ag_3		2.82	<2.64	>470
Ag_4		2.53	<2.35	>527
Ag_5		2.45	<2.27	>546
Ag_6		2.38	<2.20	>563
Ag_7		2.31	<2.13	>582

[a] Absorption data taken from ref 34.

$g_\perp = 1.974$. Consequently, the broadened $g = 1.99$ resonance in Figure 4A most probably arises from surface silver dimers that have trapped a hole, and the $g = 1.72_3$ resonance is from the intermediate case exciton that forms from close pairs of donors (shallowly trapped electrons) and acceptors (Ag_2^+ on the surface). The intermediate case exciton resonance should occur at a *g*-value that is close to the mean of the donor and acceptor (~1.75),[34] but this value will be modified by any exchange interactions. Thus, existence of a new acceptor resonance suggests that a surface silver dimer is acting as a hole trap (ionized acceptor). The similarity of the excitation spectra observed when monitoring the donor−acceptor emission and the new bands at 550 and 640 nm suggests that the active center is the same silver cluster in two environments.

Preliminary studies of oxidation of the R-sensitization centers using redox buffer solutions indicated that all the new luminescence bands were removed by buffers with potentials of +450 or +195 mV but that a buffer with a potential of −80 mV acted only on the modified 590 nm band. Recent work by Tani suggests that R-sensitization centers that are oxidized at potentials near −100 mV are hole-trapping centers while centers that are oxidized between +200 and +300 mV are electron-trapping centers.[1,35]

Nature of the Center. The spectroscopic data presented suggests that there are two closely related centers that are active and that these are centers on a {111} surface. The excitation spectra from the 550 and 640 nm emissions are identical and peak at 442 nm. The rapid decay of the 550 nm emission, after pulsed excitation and the much slower decay of the 640 nm luminescence, is suggestive of a spin-allowed and a spin-forbidden transition (singlet and triplet?) in a center that is behaving as an isolated molecular species. The excitation spectrum for the modified 590 nm donor−acceptor emission is only slightly blue-shifted, peaking at about 430 nm. This similarity of excitation spectra suggests that the center functioning as an acceptor (hole trap) and the center acting as a "molecular" species are very similar in structure. The *g*-factors in the ODMR spectra associated with the 590 nm emission suggest that this center is a silver dimer. To help confirm this assignment, the known spectroscopy of small silver clusters was examined.

The energies of the 0,0 bands in the gas phase and the peaks of the lowest absorption bands in rare gas matrices have been obtained for many of the smaller silver clusters.[36] These data are given in Table 3. The absorption spectrum of a silver cluster on an AgBr surface is expected to be shifted to longer wavelengths owing to dispersive interactions. This shift is estimated be on the order of several hundred millielectronvolts. Using 200 meV as a first estimate, upper limits to the expected peak positions on an AgBr surface are given in Table 3.

TABLE 4: Calculated and Experimental Properties of Ag and Ag_2

property	Ag cal	Ag expt	Ag_2 cal	Ag_2 expt
bond length (Å)			2.61	2.53
bond energy (eV)			1.57	1.64
ionization potential (eV)	7.75	7.57	7.81	7.56
electron affinity (eV)	1.09	1.30	0.92	1.06

These data, while approximate, suggest that the most likely candidate for the photoactive center is Ag_2. However, Ag atoms and the Ag_3 cluster should also be considered as possibilities. Silver atoms can probably be eliminated as they are known to have a very small electron binding energy in the bulk and are thought to ionize rapidly even on the silver halide surface.[5] Ag_3 might be eliminated as its lowest absorption maximum in an argon matrix is close to the 442 nm observed in the excitation spectra, and the expectation is that this peak would be significantly red-shifted for this cluster on a AgBr surface. To refine our insight into the nature of the center, computational methods have been used to predict how these centers will behave on an AgBr surface.

Computational Method. The reliability of the method of calculation including basis sets and pseudopotentials was first tested for the ground states of Ag and Ag_2. The local density method with the B3LYP functional[37,38] with the lanl2dz basis set and pseudopotential extended by one f polarization function as contained in the Gaussian 94 program was employed.[39] The results shown in Table 4 indicate a good treatment of the ground state.

We used the CIS method to calculate the excited-state energies of the closed shell ground-state systems.[40] This method was needed since rather large systems, such as Ag_2 on a small AgBr cluster, were to be treated. As is known, this method considers single excitations in a frozen-orbital approximation. Using this method, we computed 2.97 eV as the energy of the free Ag_2 excited singlet state at the equilibrium distance of 2.61 Å, which compares favorably with the experimental value of 2.85 eV.[41] At the same internuclear separation, the two lowest triplet states were calculated at 1.13 and 2.33 eV, but there are no experimental values for comparison. The goal in this first study of excited states of adsorbed silver centers is to make an assignment of the experimentally observed transitions. It is believed that our method will be sufficient for this purpose based upon the calculated singlet energy and the data in Table 4. Using the more accurate CASSCF method, previous calculations of the excited states of free Ag_2 clusters have given 1.37 and 2.68 eV for the first triplet and singlet states, respectively.[42] This more accurate method positions the second triplet (the $^3\Pi_u$ state) slightly above the first singlet state at 2.90 eV, in contrast to the CIS results given above.

The silver halide surface models used for our calculations also require some comment. The structure of the {111} surfaces are not well-established, although some modeling work underway supports a microfacetted structure containing areas of {100} surface planes.[43] Experimental work on fcc alkali halides has confirmed a microfacetted structure on a "{111}" surface, and detailed models indicate the probability of numerous kinks and double kinks in this surface.[44] Consequently, our cluster calculations have been applied to silver clusters adsorbed to a {100} AgBr surface modeled with and without the defects thought to provide sites for the clusters.[45] The flat surface consisted of a square Ag_2Br_2 unit treated quantum mechanically and embedded in a $6 \times 6 \times 6$ point-ion array. The ions were placed at sites appropriate for the AgBr crystal. Single positive

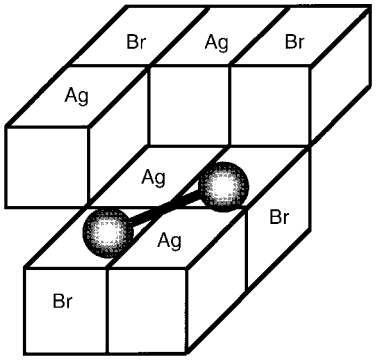

Figure 7. Diagram of the Ag_4Br_4 quantum mechanical positive kink unit that is embedded in the array of point-ions. The calculated equilibrium position of the adsorbed Ag_2 molecule is shown.

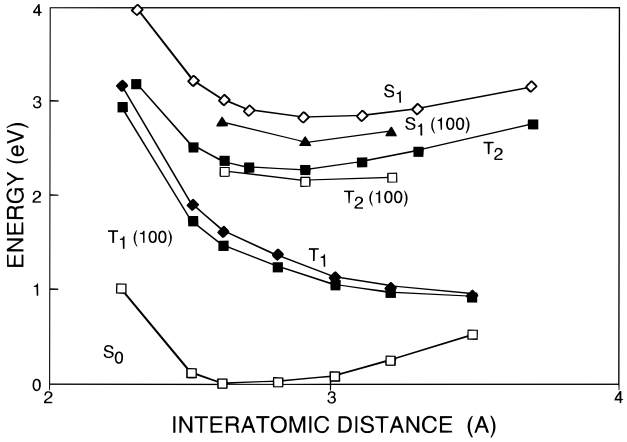

Figure 8. Calculated energy surfaces for ground state (S_0), triplet states (T_1 and T_2), and excited singlet (S_1) states of Ag_2. Curves for the S_0, T_1, and T_1 {100} states are calculated by the MP2 method, which shows better convergence to the separated atom limit. Curves for the T_2, S_1, T_2 {100}, and S_1 {100} states are calculated by the CIS method. Potential curves are shown for Ag_2 free and adsorbed to AgBr {100} surface models.

kinks (+K) were considered by adding a partial layer of point-ions to the model and treating an embedded Ag_4Br_4 quantum mechanical unit whose structure is shown in Figure 7. In the figure, we also show the optimized position of Ag_2, which was determined in earlier calculations.[45] The double-kink model, in which a second ledge of ions extends up to the kink, was treated similarly. In double kinks, a pair of positive ions is balanced by a pair of negative ions at the vicinity of the kink site, resulting in a defect that is approximately neutral in charge. In these calculations, we specifically consider the negative double kink (−DK), where the ions on the inner corner of the kink are Br ions. The analogous positive double kink (+DK) has Ag ions on the inner corner of the kink. Note that in these models the Ag_2 molecule only interacts with nearest-neighbor quantum mechanical ions, avoiding unphysical effects that may occur if the wave function penetrates into the point-ions. The Br ions were treated with the lanl2dz basis functions and pseudopotentials.

Cluster Computation Results. Using the methodologies described above, we begin with the free Ag_2 molecule and compute the ground-state and excited-state potential energy surfaces, as illustrated in Figure 8. At large internuclear separations, the ground state and first triplet state (T_1) go over to the two S states of the separated atoms, while the second triplet (T_2) and first excited singlet (S_1) separate to one S state and one P state. The first triplet state is dissociative, with the energy separation from the ground state a strong function of the internuclear separation. The second triplet has an energy minimum at 2.9 Å, where the separation from the ground state is 2.23 eV. The first singlet state also has an energy minimum at 2.9 Å and is 2.78 eV above the ground state. Note that the minimum internuclear separation for these two excited states is 0.3 Å greater than the calculated internuclear distance for the ground state using the local density method.

TABLE 5: Calculated Energy of Excited States for Ag_2 on AgBr at Different Sites[a]

site	T_1 (eV)	T_2 (eV)	S_1 (eV)
free	0.75	2.23	2.78
{100}	0.65	2.11	2.55
positive kink	0.90	1.64	2.49
negative double kink	0.96	1.54	2.33

[a] All energies at 2.9 Å internuclear separation.

We now consider the Ag_2 molecule adsorbed to various sites on the miniature AgBr {100} surface. At the present level of understanding of the structure of the {111} surface, it is felt that the various kink sites represent most of the microstructures available to the silver clusters. Several orientations of the silver dimer on a simple {100} surface were considered with the favored one having its bond at the midpoint of the center of the Ag_2Br_2 unit and its axis along {100}. In this configuration, the molecule is located at an interaction minimum at 3.0 Å above the surface. The excitation energies were added to the ground-state curve to obtain the curves for the adsorbed Ag_2. The most significant effect due to adsorption is found to be a decrease in the energy of the excited states relative to the free Ag_2 molecule. At the internuclear separation of 2.9 Å, the transition energies correspond to 2.11 and 2.55 eV, respectively, for the T_2 and S_1 states. We have repeated these calculations at the positive-kink and double-kink sites. The results are shown in Table 5. Adsorption at the positive- or double-kink sites further lowers the excited state for both S_1 and T_2. This effect is larger for the T_2 than the S_1 state.

One artifact of the CIS calculation is that the T_1 and S_0 curves appear to cross as the internuclear distance increases. This deficiency was corrected using Moller−Plesser perturbation theory (MP2) to calculate the ground and T_1 states for Ag_2 free and adsorbed to the {100} AgBr surface model. These results are shown in Figure 8 along with the CIS calculations for the T_2 and S_1 states. The MP2 method treats the S_0 and T_1 levels better at large internuclear distances. The other trends are similar to the CIS method.

The experimentally observed center has an absorption peak at 442 nm (2.81 eV) and a corresponding emission peak at 550 nm (2.25 eV). The 0,0 transition for this center, in the absence of a zero phonon line, can best be estimated at midway between the absorption and emission maxima at 2.53 eV. This value agrees best with the calculated excited singlet (S_1) states for Ag_2 on a {100} surface or at a positive kink, although the S_1 state for Ag_2 at a double kink is also a reasonable possibility, given the uncertainty in these estimates. The experimental emission peak at 640 nm (1.94 eV) would be expected to have a 0,0 transition some 0.25 eV higher in energy at ≈2.19 eV. This value lies closest to the energies calculated for the T_2 state. However, the fact that our calculation of T_2 differs significantly from the more accurate CASSCF calculations for gas-phase Ag_2 makes assignment of this emission to T_2 uncertain.

Larger closed shell silver clusters could also be a source of emission, so we performed calculations for these. For free Ag_4,

we calculate the T_1, T_2, and S_1 states at 0.43, 1.32, and 1.24 eV, respectively. Since these states are significantly lower in energy than the experimental 0,0 transition, it is reasonable to exclude Ag_4 and larger clusters from consideration as a possible source for the observed emissions. Similar calculations for Ag_3 could not be done because of the open shell nature of its ground state. However, its excited states are expected to be shifted to lower energy than in Ag_2, on the basis of experimental results measured in inert gas matrixes for these clusters.[46] Given these considerations, it is unlikely that Ag_3 is contributing to the experimentally observed emission.

The data in Tables 3 and 5 would suggest that the most probable cluster causing the new spectroscopic features is the silver dimer (Ag_2). A strong case, based on lifetimes and excitation spectra, can be made for assigning the 550 nm luminescence to an allowed molecular-like transition (S_1 to S_0?) and a weaker case for assigning the 640 nm luminescence to a forbidden molecular-like transition (T_2 to S_0?) from the same species. Excitation spectra together with ODMR studies also show that the normal AgBr donor−acceptor luminescence at ≈590 nm is changed by R-sensitization to a process that is interpreted as recombination between surface acceptors and donors that are distributed close to the surface in a manner that broadens the ODMR resonance. In addition, many of the donor acceptor pairs are close enough to form intermediate case excitons. Compared to the clusters responsible for the 550 nm emission, the ODMR active clusters have an excitation spectrum that is blue-shifted by only 0.06 eV, suggesting that these species are probably dimers also. In making this assignment, it is implied that the surface acceptors are Ag_2 clusters that trap holes. Thus, the evidence from the optical spectra are consistent with the evidence from the ODMR spectra, indicating the involvement of Ag_2^+ centers as acceptors in the modified donor−acceptor emission.

The behavior of the luminescent silver species, which are thought to be silver dimers, implies that there are constraints on the manner in which the excited states of the centers align with the conduction and valence bands of AgBr. The center that participates in donor−acceptor recombination with an excitation peak at 430 nm must have its S_1 state energetically capable of rapidly injecting an electron into the AgBr conduction band, leaving behind a hole trapped at the center. The species that is molecular-like with an absorption at 442 nm and emissions at 550 and 640 nm must either be relatively uncoupled from the lattice and/or have its S_1 state positioned so that charge injection into the AgBr valence or conduction bands is relatively slow compared to radiative relaxation from this state. The experiments with redox buffers also suggest that the center associated with the modified 590 nm donor−acceptor emission is more easily oxidized (i.e., more hole-trapping) than the center producing the 550 and 640 nm emissions. Possible alignments of the centers and their associated emissions are shown schematically in Figure 9.

Using the local density method with the BLYP functional, ionization potentials (IP) and electron affinities (EA) of Ag_2 centers on various sites have been previously calculated.[47] These values are given in Table 6 and can be used to position the energies of the various states of the centers with respect to the AgBr valence and conduction bands. To determine whether the excited singlet state of the center is energetically capable of injecting electrons into the conduction band, the singlet energy given in Table 5 is subtracted from the ionization potential of the ground state to give the ionization potential of this excited state. Similarly, to determine whether the excited singlet state has the appropriate energy to inject holes into the valence band, the singlet energy is added to the electron affinity of the ground state to give the excited state's electron affinity. Results of these calculations are included in Table 6.[48] Note that, using this calculation method, the ionization potential of an electron in the AgBr valence band is 6.2 eV and the ionization potential of an electron in the conduction band is 3.6 eV. The emphasis here is on trends in the cluster energy levels with partial charge at the absorption site. In this regard, similar behavior was also found in the calculations at different sites on the AgCl surface.[45]

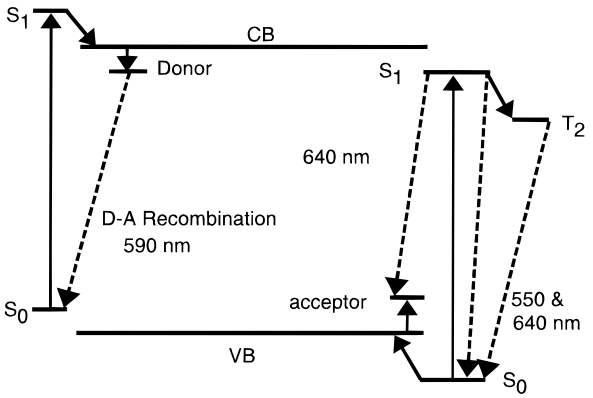

Figure 9. Schematic diagram of possible arrangements of Ag_2 ground and excited states relative to the AgBr conduction and valence bands and the resulting luminescent emission.

TABLE 6: Calculated Ionization Potentials and Electron Affinities for Ag_2 on AgBr at Different Sites

site	IP (S_0) eV	EA (S_0) eV	IP (S_1) eV	EA (S_1) eV
{100}	4.61	3.49	2.06	6.04
positive kink	6.41	4.28	3.92	6.77
negative double kink	5.35	2.56	2.97	4.94

From the values in Table 6, it can be seen that Ag_2 on a flat {100} surface is predicted to have a ground state (S_0) that will trap holes from the valence band (IP < 6.2 eV) and an excited state (S_1) that can inject electrons into the conduction band (IP < 3.6 eV). Similarly at the negative double kink, the ground state of the cluster is hole-trapping and the excited state is capable of electron injection. The positive double kink was not explicitly treated in these BLYP calculations, but earlier atomistic calculations suggest that its IP should be about 0.5 eV more positive than the negative double kink, which indicates that the hole-trapping and excited-state electron-injecting properties of both double-kink sites should be similar. Thus, any of these three neutrally charged adsorption sites gives the behavior shown on the left side of Figure 9. At the level of approximation used in our calculations it is not possible to distinguish between these three types of centers. It is expected that the observed centers are at double kinks as no centers were observable spectroscopically on microcrystals with well-formed {100} surfaces.

At the positive kink on AgBr, the calculations shown in Table 6 predict that Ag_2 has a ground state that traps electrons (EA > 3.6 eV) and an excited state that can inject holes into the valence band (EA > 6.2 eV). However, because the electron affinity of the excited state is only slightly greater than the energy of a hole in the valence band, it might be expected that hole injection from this species would be slow allowing the excited state to live long enough to give a substantial yield of radiative emission. This situation corresponds to the right side of Figure 9, where the 550 nm emission is the luminescence of the excited singlet state and the 640 nm emission is assigned

as either triplet emission or as a donor−acceptor recombination emission between the hole injected into the valence band and the electron remaining behind on the Ag_2 cluster.

The ODMR spectra confirm that the donor−acceptor recombination observed with a monitoring wavelength of 580−590 nm involves a new hole trap and a perturbed donor. With a 650 nm monitoring wavelength, changes occur in the donor resonance and a very broadened intrinsic acceptor resonance appears weakly, together with the resonances associated with the new hole trap and the intermediate case exciton. These changes are consistent with (but do not prove) the interpretation of the 640 nm band as recombination of electrons trapped at surface silver dimers with either surface-trapped holes or intrinsic acceptors. These ODMR changes do not, however, rule out some of the 640 nm emission arising from a T_2 to S_0 transition of Ag_2. That possibility may be better determined by refined future calculations of Ag_2 centers on AgBr surfaces that clarify whether the T_2 level is above or below the S_1 level for the case of adsorbed centers.

This assignment of the spectroscopically observed transitions to silver dimers at two different surface defect sites provides support for extensive previous work that has inferred the presence of such dimers from more indirect evidence.[1] The hole-trapping center formed by R-sensitization, termed an R-center by Tani,[1] has been speculated to be a silver dimer at a neutral kink site based on earlier molecular orbital calculations of Hamilton and Baetzold.[4] The same calculations were used to suggest that the electron-trapping center formed by R-sensitization, termed a P-center by Tani, is a silver dimer at a positive kink site. These electron-trapping centers have also been assumed to be Ag clusters that are essentially the same as the initial stable centers formed by light exposure (termed latent subimage). Our preliminary experiments showing that a weak 440 nm peak in the excitation spectrum can be produced by nanosecond flash exposure of AgBr tabular microcrystals are consistent with this assumption.

If we assume that the spectroscopic transitions that are observed for R-sensitized AgBr microcrystals with {111} surfaces are signatures of the centers producing enhanced photographic sensitivity, the question arises as to why these transitions are not observable for R-sensitized microcrystals with well-defined {100} surfaces. The most likely explanation is that the defects needed to produce these centers are at quite low concentration on {100} surfaces and the number produced, while sufficient for a photographic effect, is not large enough to be detected spectroscopically.

The red light irradiation studies indicate that the species associated with the 550 and 640 nm emission can be photobleached by 670 nm, but not by 780 nm irradiation. The potential energy curves given in Figure 8 (and ref 40) provide a possible explanation for this behavior. Bleaching occurs at photon energies above about 1.6 eV. This energy is sufficient for a transition from the ground state to the weakly bound or repulsive T_1 state. Absorption would create an excited Ag_2 molecule that can disassociate into two silver atoms, which, in turn, can lose electrons to the conduction band and become silver ions.

Also, wavelength-dependent latent image bleaching studies done by Hada and co-workers[49] appear to show that Ag_2 sublatent images centers can be photobleached only by wavelengths shorter than 750 nm, but larger centers such as Ag_3 and Ag_4 are photobleached at wavelengths as long as 1000 nm. If we conjecture that the photobleaching behavior of electron-trapping R-sensitization centers with size should parallel the behavior of latent subimage centers, then the photobleaching characteristics of the spectroscopically observed center responsible for the 442 nm excitation band would imply that this center is Ag_2.

Conclusions

Treatment of AgBr microcrystalline dispersions with a variety of reducing agents produces small silver centers, some of which manifest themselves by low-temperature optical emission and excitation spectra. The spectroscopically observable species are silver dimers at two different surface structures on a {111} surface: a "neutral" double kink and a positive kink. Ag_2 located at a double kink has an excitation peak at 430 nm and completely changes the intrinsic 590 nm donor−acceptor emission by creating a new surface acceptor, which is manifest in the ODMR spectrum. This ODMR evidence indicates that the silver dimer at a double kink is a hole-trapping species. Ag_2 positioned at a positive kink has an emission that is more molecular in nature with an excitation peak at 442 nm and two emission bands, which peak at 550 and ≈640 nm. The 550 nm emission has a measured lifetime of less than 10 ns and is assigned to an S_1 to S_0 transition. The emission at 640 nm with a half-life of ≈10 microseconds is more problematic. It is assigned either to a T_2 to S_0 transition or to recombination of electrons trapped at Ag_2 with holes trapped at acceptors that are either intrinsic species or dimers at double kinks. This second assignment, which is regarded as more likely, indicates that the silver dimer at positive sites is electron-trapping. Finally, a low-lying essentially repulsive triplet state is suggested as the state responsible for the observed red light bleaching of the Ag_2 centers. These assignments are supported by extensive calculations of positions and energetics of small silver clusters at various sites on silver halide surfaces.

Acknowledgment. The authors thank Joe Hodes, Sandy Finn, Laura Buonemani, Jeri Mount, and Bonnie Hein for technical support. We also thank Marian Henry and Roger Bryant for providing some of the AgBr microcrystalline dispersions. We are grateful to Ken Lushington, Ralph Young, Ray Eachus, Jeff Hansen, and Jerry Lenhard for many helpful discussions and some physical measurements.

References and Notes

(1) Tani, T. *Photographic Sensitivity*; Oxford University Press: Oxford, 1995; Chapter 4 and references therein.
(2) Harbison, J. M.; Spencer, H. E. In *The Theory of the Photographic Process*, 4th ed.; James, T. H., Ed.; Macmillan: New York, 1977; pp 151−152.
(3) Tani, T. *Photogr. Sci. Eng.* **1974,** *18*, 569.
(4) Hamilton, J. F.; Baetzold, R. C. *Photogr. Sci. Eng.* **1981,** *25*, 189.
(5) Hamilton, J. F. *Adv. Phys.* **1988,** *37*, 359.
(6) See: Hailstone, R. K.; Liebert, N. B.; Levy, M.; McCleary, R. T.; Girolmo, S. R.; Jeanmaire, D. L.; Boda, C. R. *J. Imaging Sci.* **1988,** *32*, 113 and references therein.
(7) Hailstone, R. K.; Liebert, N. B.; Levy, M.; Hamilton, J. F. Unpublished results, 1990.
(8) Tani, T. *Photogr. Sci. Eng.* **1974,** *18*, 569.
(9) Collier, S. *Photogr. Sci. Eng.* **1979,** *23*, 113.
(10) Starbova, K. *Photogr. Sci. Eng.* **1984,** *28*, 245.
(11) Tani, T. *Photographic Sensitivity*; Oxford University Press: Oxford, 1995; Chapter 6 Section 4.
(12) Kellogg, L. M.; Liebert, N. B.; James, T. H. *Photogr. Sci. Eng.* **1972,** *16*, 115.
(13) Kanzaki, H.; Tadakuma, Y. *J. Phys. Chem. Solids* **1994,** *55*, 631.
(14) Codling, A. J. B. *Photogr. Sci. Eng.* **1975,** *19*, 44.
(15) Guo, S.; Hailstone, R. K. *J. Imaging Sci. Tech.* **1996,** *40*, 210.
(16) Costa, F.; Janusonis, G. A.; Merrigan, J. A. *Photogr. Sci. Eng.* **1978**, *22*, 301.
(17) Olm, M. T. Private communication.
(18) James, T. H.; Vanselow, W.; Quirk, R. F. *PSA J.*, **1948**, *14*, 349.

(19) Berry, C. R. In *The Theory of the Photographic Process;* James, T. H., Ed. Macmillan: New York, 1977; Chapter 3; U.S. Patent Number 5,147,771 Sept 15, 1992; U.S. Patent Number 5,210,013, May 11, 1993.
(20) James, T. H.; Vanselow, W.; Quirk, R. F. *Photogr. Sci. Technol.* **1953,** *19B,* 170.
(21) Marchetti, A. P.; Johannsson, K. P.; McLendon, G. L. *Phys. Rev. B* **1993,** *47,* 4268.
(22) Marchetti, A. P.; Burberry, M. S.; Spoonhower, J. P. *Phys. Rev. B* **1991,** ***43****,* 2378.
(23) Czaja, W.; Baldereschi, A. *J. Phys. C* **1979,** *12,* 405.
(24) Marchetti, A. P.; Burberry, M. S. *Phys. Rev. B* **1988,** ***37****,* 10862.
(25) Burki, Y.; Czaja, W. *Europhys. Lett.* **1989,** *10,* 55.
(26) Burberry, M. S. Marchetti, A. P. *Phys. Rev. B* **1985**, *32,* 1192.
(27) Moser, F.; Lyu, S. *J. Luminescence*, **1971,** *3,* 447.
(28) Tani, T. *Photogr. Sci. Eng.* **1971**, *15,* 181.
(29) Babcock, T. A.; Ferguson, P. M.; Lewis, W. C.; James, T. H. *Photogr. Sci. Eng.* **1975,** *19,* 49. James, T. H. In *The Theory of the Photographic Process*, 4th ed.; James, T. H., Ed.; Macmillan: New York 1977; p 164. Janusonis, G. A. *Photogr. Sci. Eng.* **1978,** *22,* 297.
(30) Klaus, R. L.; et al. U.S. Patent Number 5,219,721, June 15, 1993.
(31) Allen, C. F. U.S. Patent 2728663, Dec 27, 1955.
(32) The red light destruction of the R-sensitization spectroscopic signatures appears to be very similar to the Herschel effect. See: Bacon, R. E. In *The Theory of the Photographic Process*, 4th ed.; James, T. H. Ed., Macmillan: New York, 1977; pp 182−193.
(33) Shields, L.; Symons, M. R. C. *Mol. Phys.* **1966**, *11,* 57. Eachus, R. S.; Symons, M. R. C. *J. Chem. Soc.* A **1970**, 1329.
(34) Davies, J. J.; Nicholls, J. E. *J. Phys. C* **1982,** *15,* 5321.
(35) Tani, T. *Paper Summary Book, International East-West Symposium III,* Maui, HI, November, 1992; p A-11.
(36) Beutel, V.; Bohm, H.-J.; Demtroder, W.; Eckel, H.-A.; Gress, J. Kuhn M.; A. Sasso, A. *Laser Chem.* **1991,** *11,* 209. Harbich, W.; Fedrigo, S.; Meyer, F.; Lindsay, D. M.; Lignieres, J.; Rivoal, J. C.; Kreisle, D. *J. Chem. Phys.* **1990,** *93,* 8535. Ketter, U. L.; Bechthold, P. S.; Krasser, W. In *Physics and Chemistry of Small Clusters*; Jena, P., Rao, B. K., Khanna, S. N., Eds.; NATO ASI Series B 158; 1986; p 589. Morse, M. D. *Chem Rev.* **1986,** ***86***,1049.
(37) Becke, A. D. *Phys. Rev. A* **1988,** *38,* 3098.
(38) Lee, C.; Yang, W.; Parr, R. G. *Phys. Rev. B* **1988**, *37,* 785.
(39) Frisch, M. J.; Trucks, G. W.; Schlegel, H. B.; Gill, P. M. W.; Johnson, B. G.; Robb, M. A.; Cheeseman, J. R.; Keith, T. A.; Petersson, G. A.; Montgomery, J. A.; Raghavachari, K.; Al-Laham, M. A.; Zakrzewski, V. G.; Ortiz, J. V.; Foresman, J. B.; Cioslowski, J.; Stefanov, B. B.; Nanayakkara, A.; Challacombe, M.; Peng, C. Y.; Ayala, P. Y.; Chen, W.; Wong, M. W.; Andres, J. L.; Replogle, E. S.; Gomperts, R.; Martin, R. L.; Fox, D. J.; Binkley, J. S.; Defrees, D. J.; Baker, J.; Stewart, J. P.; Head-Gordon, M.; Gonzalez, C.; Pople, J. A. *Gaussian 94*, Revision D.4; Gaussian, Inc.: Pittsburgh, PA, 1995.
(40) Foresman, J. B.; Head-Gordon, M.; Pople, J. A.; Frisch, M. J. *J. Chem. Phys*. **1992,** *96,* 135.
(41) Simard, B.; Hackett, P. A. *Chem. Phys. Lett.* **1991,** *186,* 415.
(42) Zhang, H.; Balasubramanian, K. *J. Chem. Phys.* **1993,** *98,* 7092.
(43) Baetzold, R. C.; Hansen, J. Unpublished results.
(44) Knoppik, D.; Losch, A. *J. Cryst. Growth* **1976,** *34,* 332. Van Der Voort, E.; Hartman, P. *J. Cryst. Growth* **1990,** *104,* 450.
(45) Baetzold, R. C. *J. Phys. Chem. B* **1997,** *101,* 8180.
(46) Fedrigo, S.; Harbich, W.; Buttet, J. *J. Chem. Phys.* **1993,** *99,* 5712.
(47) Baetzold, R. C. Submitted to *J. Imaging Sci. Technol.*
(48) The values for ionization potential and electron affinity calculated for the S_0 state include terms for relaxation of the final state and are the relevant values for thermal trapping processes. A more accurate calculation appropriate for the initial charge-transfer processes from the optically excited S_1 state would exclude this relaxation but is beyond the scope of the current investigations.
(49) Kawasaki, M.; Tsujimura, Y.; Hada, H. *Phys. Rev. Lett.*, **1986,** *57,* 2796.